An Experimental Study of Dynamic Visual Feedback Control on SICE–DD Arm

Hiroyuki Kawai*, Toshiyuki Murao* and Masayuki Fujita*

* Department of Electrical and Electronic Engineering
Kanazawa University
Kodatsuno 2-40-20, Kanazawa 920-8667,Japan
fujita@t.kanazawa-u.ac.jp

Abstract: In this paper, we consider the relative rigid body motion control problem with manipulator dynamics using visual information. Firstly the model of the relative rigid body motion and nonlinear observer are described in order to derive the dynamic visual feedback system. Secondly we propose the dynamic visual feedback control law which is based on passivity. Local asymptotic stability of the overall closed-loop system and L_2-gain performance analysis for the proposed control law are discussed using the energy function. Finally experimental results on SICE–DD arm are reported to confirm the effectiveness of the visual feedback control control law.

Keywords: Visual Feedback Control, SICE–DD Arm, Lyapunov Stability, L_2–Gain Performance Analysis

1. Introduction

Vision based control of robotic systems involves the fusion of robot kinematics, dynamics, and computer vision system to control the position of the robot end-effector in an efficient manner. The combination of mechanical control with visual information, so-called *visual feedback control* or *visual servo*, should become extremely important, when we consider a mechanical system working under *dynamical* environments[1, 2]. Recently, autonomous injection of biological cells has been discussed using visual feedback control[3] and fields which need visual feedback control are increasing.

This paper deals with a robot motion control with visual information in the eye-in-hand configuration as depicted in Fig. 2. Classical visual servoing algorithms assume that the manipulator dynamics is negligible and do not interact with the visual feedback loop. However, this assumption is invalid for high speed tasks, while it holds for kinematic control problems[4].

In this paper, we discuss dynamic visual feedback control for the Eye-in-hand visual feedback system with robot manipulator depicted in Fig. 1. The main contribution of this paper is that dynamic visual feedback system with SICE–DD arm[5] is constructed in order to confirm the effectiveness of our researches[6, 7].

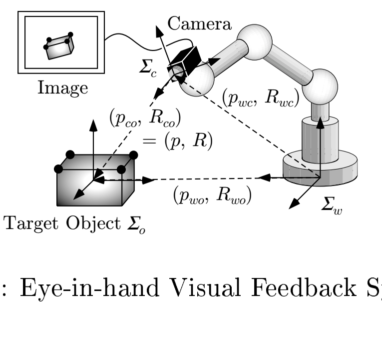

Figure 1: Eye-in-hand Visual Feedback System.

2. Modeling

2.1 Relative Rigid Body Motion Model

We consider the eye-in-hand system[1] depicted in Fig. 1, where the coordinate frame Σ_w represents the world frame, Σ_c represents the camera (end-effector) frame, and Σ_o represents the object frame, respectively. Let $p_{co} \in \mathcal{R}^3$ and $R_{co} \in \mathcal{R}^{3\times 3}$ denote the position vector and the rotation matrix from the camera frame Σ_c to the object frame Σ_o. Then, the relative rigid body motion from Σ_c to Σ_o can be represented by $(p_{co}, R_{co}) \in SE(3)$. Similarly, we will define the rigid body motion (p_{wc}, R_{wc}) from Σ_w to Σ_c, and (p_{wo}, R_{wo}) from Σ_w to Σ_o, respectively, as in Fig. 1.

The objective of the visual feedback control is to bring the actual relative rigid body motion (p_{co}, R_{co}) to a given reference (p_d, R_d) (see, e.g. reference[1]). Our goal is to determine the camera's motion via the visual information for this purpose. The reference (p_d, R_d) for the rigid motion (p_{co}, R_{co}) is assumed to be constant in the paper.

In this subsection, let us derive a model of the relative rigid body motion. The rigid body motion (p_{wo}, R_{wo}) of the target object, relative to the world frame Σ_w, is given by

$$p_{co} = R_{wc}^T(p_{wo} - p_{wc}) \tag{1}$$
$$R_{co} = R_{wc}^T R_{wo}. \tag{2}$$

The dynamic model of the relative rigid body motion involves the velocity of each rigid body. To this aid, let us consider the velocity of a rigid body as described in reference[8]. Let $\hat{\omega}_{wc}$ and $\hat{\omega}_{wo}$ denote the instantaneous body angular velocities from Σ_w to Σ_c, and from Σ_w to Σ_o, respectively. Here '$\wedge$' (wedge) is the operator from $\mathcal{R}^3$ to the set of 3×3 skew-symmetric matrices $so(3)$ [8] (Chap.2, eq.(2.4)). The operator '$\vee$' (vee) denotes

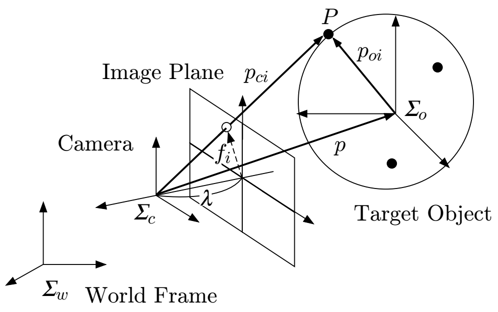

Figure 2: Pinhole camera

the inverse operator to '$\wedge$': i.e., $so(3) \to \mathcal{R}^3$. Recall that a skew-symmetric matrix corresponds to an axis of rotation (via the mapping $a \mapsto \hat{a}$). With these, it is possible to specify the velocities of each rigid body as follows[8] (Chap.2, eq.(2.55)).

$$\dot{p}_{wc} = R_{wc} v_{wc}, \quad \dot{R}_{wc} = R_{wc}\hat{\omega}_{wc} \tag{3}$$

$$\dot{p}_{wo} = R_{wo} v_{wo}, \quad \dot{R}_{wo} = R_{wo}\hat{\omega}_{wo}. \tag{4}$$

Differentiating (1) and (2) with respect to time, we can obtain

$$\dot{p}_{co} = -v_{wc} + \hat{p}_{co}\omega_{wc} + R_{co} v_{wo} \tag{5}$$

$$\dot{R}_{co} = -\hat{\omega}_{wc} R_{co} + R_{co}\hat{\omega}_{wo}. \tag{6}$$

Now, let us denote the body velocity of the camera relative to the world frame Σ_w as $V_{wc} := [v_{wc}^T \ \omega_{wc}^T]^T$. Further, the body velocity of the target object relative to Σ_w should be denoted as $V_{wo} := [v_{wo}^T \ \omega_{wo}^T]^T$. Then we can rearrange the above eqs. (5) and (6) in a matrix form as follows[7].

$$\begin{bmatrix} \dot{p} \\ (\dot{R}R^T)^\vee \end{bmatrix} = \begin{bmatrix} -I & \hat{p} \\ 0 & -I \end{bmatrix} V_{wc} + \begin{bmatrix} R & 0 \\ 0 & R \end{bmatrix} V_{wo}. \tag{7}$$

Here (p, R) denotes (p_{co}, R_{co}) for short. The eq. (7) should be the model of the relative rigid body motion.

Next let us derive a model of a pinhole camera as shown in Fig. 2. Let λ be a focal length. Let p_{oi} and p_{ci} be coordinates of the target object's i-th feature point relative to Σ_o and Σ_c, respectively. Using a transformation of the coordinates, we have

$$p_{ci} = p + R p_{oi}. \tag{8}$$

The perspective projection of the i-th feature point onto the image plane gives us the image plane coordinate f_i as follows.

$$f_i = \frac{\lambda}{z_{ci}} \begin{bmatrix} x_{ci} \\ y_{ci} \end{bmatrix} \tag{9}$$

where $p_{ci} := [x_{ci} \ y_{ci} \ z_{ci}]^T$.

2.2 Observer Model

The visual feedback control task should require information of the relative rigid body motion (p, R). However, the measurable information is only the one of image in the visual feedback systems. Hence, we consider a nonlinear observer which estimates the relative rigid body motion using information of the image.

First, we shall consider the following dynamic model which just comes from the actual relative rigid body motion model (7).

$$\begin{bmatrix} \dot{\bar{p}} \\ (\dot{\bar{R}}\bar{R}^T)^\vee \end{bmatrix} = \begin{bmatrix} -I & \hat{\bar{p}} \\ 0 & -I \end{bmatrix} V_{wc} + \begin{bmatrix} \bar{R} & 0 \\ 0 & \bar{R} \end{bmatrix} u_e \tag{10}$$

where $(\bar{p}, \bar{R})$ is the estimated value of the relative rigid body motion. The new input u_e is to be determined in order to converge the estimated value to the actual relative rigid body motion. Based on the structures of (8)(9), the estimated image information $\bar{f}_i$ are described as follows

$$\bar{f}_i = \frac{\lambda}{\bar{z}_{ci}} \begin{bmatrix} \bar{x}_{ci} \\ \bar{y}_{ci} \end{bmatrix}. \tag{11}$$

Now, we define the estimation error between the estimated value $(\bar{p}, \bar{R})$ and the actual relative rigid motion (p, R) as

$$(p_{ee}, R_{ee}) := (\bar{R}^T(p - \bar{p}), \bar{R}^T R). \tag{12}$$

Note that, if $p = \bar{p}$ and $R = \bar{R}$, then it follows $p_{ee} = 0$ and $R_{ee} = I$. Let

$$e_R(R) := \frac{1}{2}(R - R^T)^\vee \tag{13}$$

represent an error vector of the rotation matrix R. Using the notation $e_R(R)$, the vector of the estimation error is given by

$$e_e := \begin{bmatrix} p_{ee}^T & e_R^T(R_{ee}) \end{bmatrix}^T. \tag{14}$$

It should be noted that $e_e = 0$ provided $p_{ee} = 0$ and $R_{ee} = I$.

Next, we will derive a relation between the image information from the camera and the estimated image information. It is straightforward to extend the image information f_i, $\bar{f}_i$ to the m image points case by simply stacking the vectors of the image plane coordinate, i.e. $f := [f_1^T \ \cdots \ f_m^T]^T \in \mathcal{R}^{2m}$, $\bar{f} := [\bar{f}_1^T \ \cdots \ \bar{f}_m^T]^T \in \mathcal{R}^{2m}$. Then, the relation between f and $\bar{f}$ is derived as follows[7].

$$f - \bar{f} = J(\bar{g}) e_e \tag{15}$$

where

$$J(\bar{g}) := \begin{bmatrix} J_1(\bar{g}) \\ \vdots \\ J_m(\bar{g}) \end{bmatrix} \begin{bmatrix} \bar{R} & 0 \\ 0 & \bar{R} \end{bmatrix} \tag{16}$$

$$J_i(\bar{g}) := \begin{bmatrix} \frac{\lambda}{\bar{z}_{ci}} & 0 & -\frac{\lambda \bar{x}_{ci}}{\bar{z}_{ci}^2} \\ 0 & \frac{\lambda}{\bar{z}_{ci}} & -\frac{\lambda \bar{y}_{ci}}{\bar{z}_{ci}^2} \end{bmatrix} \begin{bmatrix} I & -(\bar{R}p_{oi})^\wedge \end{bmatrix}$$

$$i = 1, \cdots, m.$$

If $J(\bar{g})$ hold a full column rank, then the pseudo-inverse matrix $J(\bar{g})^\dagger$ exists and the following relation holds.

$$J(\bar{g})^\dagger(f - \bar{f}) = e_e. \tag{17}$$

We consider the state equation of the estimated relative rigid body motion error. Using (7), (10) and (12), the state equation of the estimated RRBM error can be obtained as follows.

$$\begin{bmatrix} \dot{p}_{ee} \\ (\dot{R}_{ee}R_{ee}^T)^\vee \end{bmatrix} = \begin{bmatrix} -I & \hat{p}_{ee} \\ 0 & -I \end{bmatrix} u_e + \begin{bmatrix} R_{ee} & 0 \\ 0 & R_{ee} \end{bmatrix} V_{wo}. \tag{18}$$

Since the camera velocity V_{wc} is considered as an input, the notation u_c is used instead of V_{wc}.

2.3 Visual Feedback System

Let us derive a model of the visual feedback system. First, we define the relative rigid body motion error which represents the error between the estimated value $(\bar{p}, \bar{R})$ and the reference of the relative rigid body motion (p_d, R_d) as follows.

$$(p_{ec}, R_{ec}) := (R_d^T(\bar{p} - p_d), R_d^T\bar{R}) \tag{19}$$

It should be remarked that $p_d = \bar{p}$ and $R_d = \bar{R}$ iff $p_{ec} = 0$ and $R_{ec} = I$.

Using the notation $e_R(R)$, the vector of the RRBM error is defined as

$$e_c := \begin{bmatrix} p_{ec}^T & e_R^T(R_{ec}) \end{bmatrix}^T. \tag{20}$$

Note that $e_c = 0$ iff $p_{ec} = 0$ and $R_{ec} = I$.

From (10) and (19), the state equation of the RRBM error can be given by

$$\begin{bmatrix} \dot{p}_{ec} \\ (\dot{R}_{ec}R_{ec}^T)^\vee \end{bmatrix} = \begin{bmatrix} -R_d^T & R_d^T\hat{\bar{p}} \\ 0 & -R_d^T \end{bmatrix} u_c + \begin{bmatrix} R_{ec} & 0 \\ 0 & R_{ec} \end{bmatrix} u_e. \tag{21}$$

Using (18) and (21), the state equation of the visual feedback system can be derived as

$$\begin{bmatrix} \dot{p}_{ec} \\ (\dot{R}_{ec}R_{ec}^T)^\vee \\ \dot{p}_{ee} \\ (\dot{R}_{ee}R_{ee}^T)^\vee \end{bmatrix} = \begin{bmatrix} -R_1^TB^T(\bar{p}) & R_2 \\ 0 & -B^T(p_{ee}) \end{bmatrix} \begin{bmatrix} u_c \\ u_e \end{bmatrix} + \begin{bmatrix} 0 \\ R_3 \end{bmatrix} V_{wo} \tag{22}$$

where $R_1 := \mathrm{diag}\{R_d, R_d\}$, $R_2 := \mathrm{diag}\{R_{ec}, R_{ec}\}$, $R_3 := \mathrm{diag}\{R_{ee}, R_{ee}\}$ and

$$B(a) = \begin{bmatrix} I & 0 \\ \hat{a} & I \end{bmatrix}, \quad \forall a \in \mathcal{R}^3.$$

Let us define the error vector of the visual feedback system as

$$e := \begin{bmatrix} e_c^T & e_e^T \end{bmatrix}^T \tag{23}$$

which consists of the RRBM error vector e_c and the estimated RRBM error vector e_e. It should be noted that the actual relative rigid body motion (p, R) tends to the reference (p_d, R_d) when $e \to 0$.

Lemma 1 [7] If $V_{wo} = 0$ and $e(0) = 0$, then the system (22) satisfies

$$\int_0^T u_{ce}^T \nu_{ce} d\tau \geq 0, \quad \forall T > 0 \tag{24}$$

where $u_{ce} := [u_c^T \ u_e^T]^T$ and ν_{ce} is

$$\nu_{ce} := \begin{bmatrix} -B(p_d)R_1 & 0 \\ R_2^T & -I \end{bmatrix} e. \tag{25}$$

(Proof) Consider the following positive definite function

$$W = \frac{1}{2}\|p_{ec}\|^2 + \phi(R_{ec}) + \frac{1}{2}\|p_{ee}\|^2 + \phi(R_{ee}) \tag{26}$$

where ϕ is the error function of the rotation matrix. Let us introduce the notation of the error function

$$\phi(R) := \frac{1}{2}\mathrm{tr}(I - R). \tag{27}$$

The error function ϕ has the following properties.[9]

(1) $\phi(R) = \phi(R^T) \geq 0$ and $\phi(R) = 0$ iff $R = I$.
(2) $\dot{\phi}(R) = e_R^T(R)(R^T\dot{R})^\vee = e_R^T(R)(\dot{R}R^T)^\vee$.

The positive definiteness of the function W can be given by the property of the error function ϕ. Differentiating (26) with respect to time yields

$$\begin{aligned} \dot{W} &= e^T \begin{bmatrix} \dot{p}_{ec} \\ (\dot{R}_{ec}R_{ec}^T)^\vee \\ \dot{p}_{ee} \\ (\dot{R}_{ee}R_{ee}^T)^\vee \end{bmatrix} \\ &= e^T \begin{bmatrix} -R_1^TB^T(\bar{p}) & R_2 \\ 0 & -B^T(p_{ee}) \end{bmatrix} u_{ce}. \end{aligned} \tag{28}$$

Observing that the skew-symmetry of the matrices $\hat{p}_{ec}$ and $\hat{p}_{ee}$, i.e. $p_{ec}^T\hat{p}_{ec}\omega_{wc} = -p_{ec}^T\hat{\omega}_{wc}p_{ec} = 0$ and $p_{ee}^T\hat{p}_{ee}\omega_{wc} = -p_{ee}^T\hat{\omega}_{wc}p_{ee} = 0$, the above equation along the trajectories of the system (22) can be transformed into

$$\begin{aligned} \dot{W} &= e^T \begin{bmatrix} -R_1^TB^T(p_d) & R_2 \\ 0 & -I \end{bmatrix} u_{ce} \\ &= u_{ce}^T \nu_{ce}. \end{aligned} \tag{29}$$

Integrating (29) from 0 to T, we can obtain

$$\int_0^T u_{ce}^T \nu_{ce} d\tau = W(e(T)) - W(e(0)) \geq 0. \tag{30}$$

This completes the proof. □

In the visual feedback system (22), $p_{ec}^T\hat{\omega}_{wc}p_{ec} = 0$ and $p_{ee}^T\hat{\omega}_{wc}p_{ee} = 0$ hold. This property is analogous to the one of the robot dynamics, i.e. $x^T(\dot{M} - 2C)x = 0$, $\forall x \in \mathcal{R}^m$ (where $M \in \mathcal{R}^{n\times n}$ is the manipulator inertia matrix and $C \in \mathcal{R}^{n\times n}$ is the Coriolis matrix[8]). Moreover, let us take u_{ce} as the input and ν_{ce} as its output. Then, Lemma 1 would suggest that the system (22) is *passive* from the input u_{ce} to the output ν_{ce} just formally as in the definition in the reference[10]. Fig. 3 shows a block diagram of the visual feedback system.

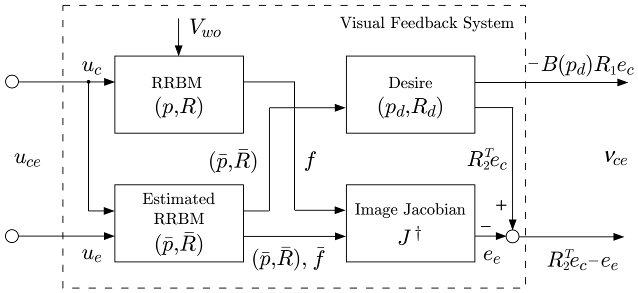

Figure 3: Block diagram of visual feedback system.

2.4 Dynamic Visual Feedback System

The manipulator dynamics can be written as

$$M(q)\ddot{q} + C(q,\dot{q})\dot{q} + g(q) = \tau \tag{31}$$

where q, $\dot{q}$ and $\ddot{q}$ are the joint angles, velocities and accelerations, respectively. τ is the vector of the input torques.

Here we propose the control law as the input torques for the dynamic visual feedback system as follows.

$$\begin{aligned}\tau = M(q)\ddot{q}_d + C(q,\dot{q})\dot{q}_d + g(q)\\ +J_b^T(q)B(p_d)R_1e_c + u_\xi\end{aligned} \tag{32}$$

where $\dot{q}_d$ and $\ddot{q}_d$ are references of joint velocities and accelerations, respectively. $J_b(q)$ is the manipulator body Jacobian[8] and the new input u_ξ is to be determined in order to achieve the control objectives.

Let us define the error vector with respect to the joint velocities of the manipulator dynamics as $\xi := \dot{q} - \dot{q}_d$. Here we consider the error dynamics of the manipulator. Substituting (32) into (31) yields

$$M(q)\dot{\xi} = -C(q,\dot{q})\xi + J_b^T(q)B(p_d)R_1e_c + u_\xi. \tag{33}$$

Since the camera is mounted on the end-effector of the manipulator in the eye-in-hand configuration, the body velocity of the camera V_{wc} is given by

$$V_{wc} = J_b(q)\dot{q}. \tag{34}$$

Similarly, let u_d represent a reference of the velocity of the end-effector, then $u_d = J_b(q)\dot{q}_d$ holds.

Using eqs. (22), (33) and (34), the state equation of the dynamic visual feedback system can be derived as

$$M(q)\dot{\xi} = -C(q,\dot{q})\xi + J_b^T(q)B(p_d)R_1e_c + u_\xi \tag{35}$$

$$\begin{aligned}\begin{bmatrix}\dot{p}_{ec}\\(\dot{R}_{ec}R_{ec}^T)^\vee\\\dot{p}_{ee}\\(\dot{R}_{ee}R_{ee}^T)^\vee\end{bmatrix} = \begin{bmatrix}-R_1^TB^T(\bar{p})\\0\end{bmatrix}J_b(q)\xi + \begin{bmatrix}0\\R_3\end{bmatrix}V_{wo}\\ +\begin{bmatrix}-R_1^TB^T(\bar{p}) & R_2\\0 & -B^T(p_{ee})\end{bmatrix}\begin{bmatrix}u_d\\u_e\end{bmatrix}.\end{aligned} \tag{36}$$

Let us define the error vector of the dynamic visual feedback system as

$$x := \begin{bmatrix}\xi^T & e^T\end{bmatrix}^T \tag{37}$$

which consists of the error vector of the joint velocities ξ and the error vector of the visual feedback system e.

3. Dynamic Visual Feedback Control

In this section, we propose the dynamic visual feedback control law which guarantees local asymptotic stability of the overall closed-loop system. Before deriving the control law, we show an important lemma.

Lemma 2 If $V_{wo} = 0$ and $x(0) = 0$, then the system (35)(36) satisfies

$$\int_0^T u^T\nu d\tau \geq 0,\quad \forall T > 0 \tag{38}$$

where $u := [u_\xi^T\ u_d^T\ u_e^T]^T$ and ν is

$$\nu := \begin{bmatrix}I & 0 & 0\\0 & -B(p_d)R_1 & 0\\0 & R_2^T & -I\end{bmatrix}x. \tag{39}$$

(Proof) Consider the following positive definite function

$$\begin{aligned}V = \frac{1}{2}\xi^TM\xi + \frac{1}{2}\|p_{ec}\|^2 + \phi(R_{ec})\\ +\frac{1}{2}\|p_{ee}\|^2 + \phi(R_{ee}).\end{aligned} \tag{40}$$

Differentiating (40) with respect to time yields

$$\dot{V} = \xi^TM\dot{\xi} + \frac{1}{2}\xi^T\dot{M}\xi + e^T\begin{bmatrix}\dot{p}_{ec}\\(\dot{R}_{ec}R_{ec}^T)^\vee\\\dot{p}_{ee}\\(\dot{R}_{ee}R_{ee}^T)^\vee\end{bmatrix} \tag{41}$$

Observing that the skew-symmetry of the matrices $\dot{M}-2C$, $\hat{p}_{ec}$ and $\hat{p}_{ee}$, i.e. $\xi^T(\dot{M}-2C)\xi = 0$, $p_{ec}^T\hat{p}_{ec}\omega_{wc} = -p_{ec}^T\hat{\omega}_{wc}p_{ec} = 0$ and $p_{ee}^T\hat{p}_{ee}\omega_{wc} = -p_{ee}^T\hat{\omega}_{wc}p_{ee} = 0$, the above equation along the trajectories of the system (35)(36) can be transformed into

$$\dot{V} = \xi^Tu_\xi + e^T\begin{bmatrix}-R_1^TB^T(p_d) & R_2\\0 & -I\end{bmatrix}\begin{bmatrix}u_d\\u_e\end{bmatrix} = u^T\nu. \tag{42}$$

Integrating (42) from 0 to T, we can obtain

$$\int_0^T u^T\nu d\tau = V(x(T)) - V(x(0)) \geq 0. \tag{43}$$

This completes the proof. □

Fig. 4 shows a block diagram of the dynamic visual feedback system.

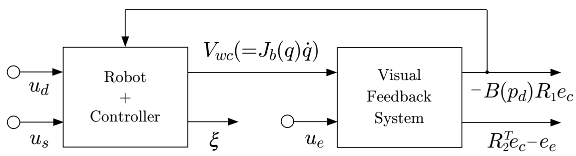

Figure 4: Block diagram of dynamic visual feedback system.

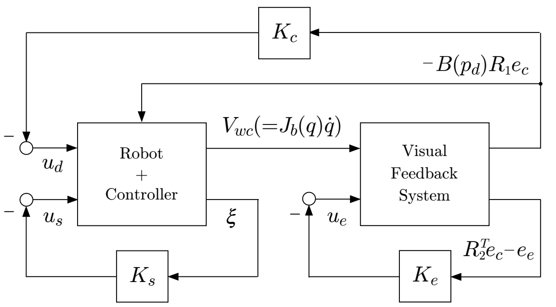

Figure 5: Block diagram of dynamic visual feedback control.

It is well known that there is a direct link between passivity and Lyapunov stability. Thus, we propose the following control input.

$$u = -\begin{bmatrix} K_\xi & 0 & 0 \\ 0 & K_c & 0 \\ 0 & 0 & K_e \end{bmatrix} \nu \tag{44}$$

where K_ξ is $n \times n$ positive definite matrix, K_c and K_e are 6×6 positive definite matrices.

The result with respect to asymptotic stability of the proposed control input (44) can be established as follows.

Theorem 1 [6] If $V_{wo} = 0$, then the equilibrium point $x = 0$ for the closed-loop system (35)(36) and (44) is asymptotically stable.

(Proof) See the reference[6]. □

The block diagram of the dynamic visual feedback control is shown in Fig. 5.

We consider L_2-gain performance analysis of the visual feedback system. Now, let us define

$$P := K_\xi - \frac{1}{2}I, \quad Q := K_{ce} - \frac{1}{2}\begin{bmatrix} I & 0 \\ 0 & (1+\frac{1}{\gamma^2})I \end{bmatrix}$$

where $\gamma \in \mathcal{R}$ is positive and

$$K_{ce} := \begin{bmatrix} -R_1^T B^T(p_d) & R_2 \\ 0 & -I \end{bmatrix} \begin{bmatrix} K_c & 0 \\ 0 & K_e \end{bmatrix} \begin{bmatrix} -B(p_d)R_1 & 0 \\ R_2^T & -I \end{bmatrix}.$$

Then we have the following theorem.

Theorem 2 [6] Given a positive scalar γ and consider the control input (44) with the gains K_ξ, K_c and K_e such that the matrices P and Q are positive semi-definite, then the closed-loop system (35), (36) and (44) has L_2-gain $\leq \gamma$.

(Proof) See the reference[6]. □

Lemma 2 can be interpreted as follows. The dynamic visual feedback system (35) (36) is *passive* from the input u to the output ν just formally as in the definition in the reference[10]. The positive definite function V plays the role of a Lyapunov function and a storage function in Theorem 1 and 2, respectively.

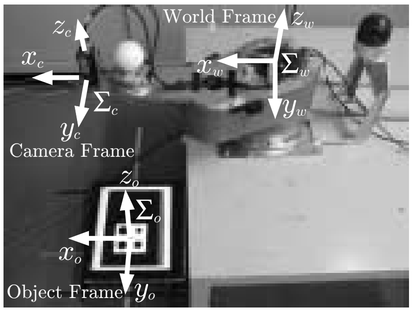

Figure 6: Experimental Arm.

4. Experimental Case Study

The manipulator use in the study, known as SICE–DD arm (see Fig. 6), is controlled by a digital signal processor(DSP) from dSPACE Inc., which utilizes a powerPC 750 running at 480 MHz. Control programs are written in MATLAB and SIMULINK, and implemented on the DSP using the Real–Time Workshop and dSPACE Software which includes ControlDesk, Real–Time Interface and so on. A PULNiX TM-7EX camera was attached at the arm tip. The video signals is acquired by a frame graver board PicPort–Stereo–H4D and a image processing software HALCON.

We defined the three coordinates which were described in Fig. 6. Let the target object have four feature points which are projected on the display and move as the following:

$Translation : (0 \leq t \leq 8)$

$x = 0.47[\mathrm{m}],\ y = 0.1 \sim -0.044[\mathrm{m}],\ z = -0.90[\mathrm{m}]$

$Rotation : (0 \leq t \leq 8)$

$x = 0^\circ,\ y = 0^\circ,\ z = 0^\circ \sim -20^\circ$

The experimental tests were carried out with the following initial configuration: $e_c(0) = e_e(0) = 0$, $q_1(0) = 30^\circ$, $q_2(0) = -30^\circ$, and $\dot{q}_1(0) = \dot{q}_2(0) = 0$. In this study, we set a reference of position and rotation as $p_d = [0\ 0\ -0.9]^T$, $R_d = I$. Then, we would like to bring the actual relative rigid body motion (p, R) to the reference (p_d, R_d).

Control gain of the manipulator is chosen as $K_\xi = \mathrm{diag}\{10, 5\}$ and gains K_c and K_e are chosen as follows

Gain A : $K_c = \mathrm{diag}\{12, 12, 8, 8, 8, 12\},\ K_e = 6I$

Gain B : $K_c = \mathrm{diag}\{30, 30, 20, 20, 20, 30\},\ K_e = 30I.$

The closed-loop (35)(36) and (44) with gain A has $\gamma = 0.522$ and gain B has $\gamma = 0.264$.

Fig. 7 and 8 present the control error vectors e_c and the estimation error vectors e_e, top graph, middle one and bottom one shows the error of translation of x, the error of translation of y and the error of rotation of z, respectively. In these figures, dashed lines denote the error of a case of gain A and solid lines denote the error of a case of gain B. Fig. 9 shows the norm of x defined

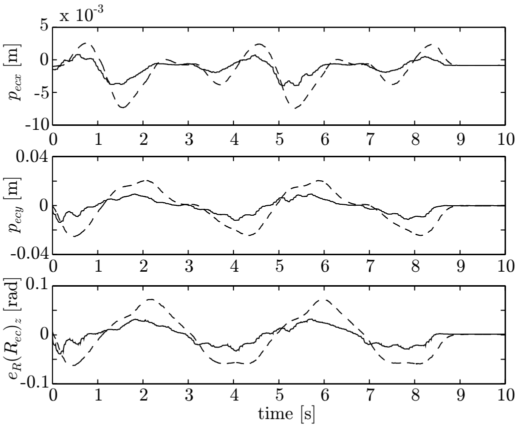

Figure 7: Control error e_c.

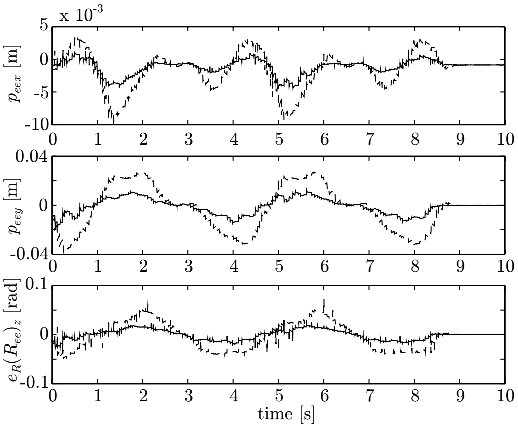

Figure 8: Estimation error e_e.

in the eq. (37). Top graph and bottom one shows the norm of the case of gain A and gain B, respectively.

In the case of the static target object, i.e. after $t = 8$ [s], all errors in Fig. 7, 8 and 9 tend to zero. It can be concluded that the equilibrium point is asymptotically stable if the target object is static. In the case of $\gamma = 0.264$, the performance is improved as compared to the case of $\gamma = 0.522$. After all, the experiment results show that L_2-gain is adequate for the performance measure of the visual feedback control.

5. Conclusion

This paper has discussed the relative rigid body motion control problem with manipulator dynamics using visual information. Firstly the model of the relative rigid body motion and nonlinear observer are described in order to derive the dynamic visual feedback system. Secondly we proposed the dynamic visual feedback control law which is based on passivity. Local asymptotic stability of the overall closed-loop system and L_2-gain performance analysis for the proposed control law has been discussed using the energy function. Finally experimental results on SICE–DD arm have been reported to confirm the effectiveness of the visual feedback control law.

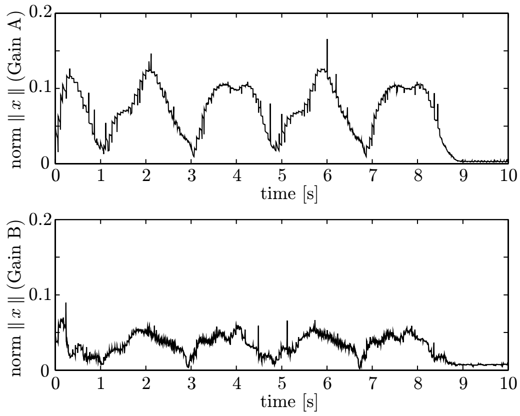

Figure 9: Norm of Error $\|x\|$.

References

[1] S. Hutchinson, G. D. Hager and P. I. Corke, "A Tutorial on Visual Servo Control," *IEEE Trans. Robotics and Automation*, vol. 12, no. 5, pp. 651–670, 1996.

[2] Mini Special Issue, "Visual Servoing," *Journal of SICE*, vol. 40, no. 9, 2001.

[3] S. Yu and B. J. Nelson, "Autonomous Injection of Biological Cells Using Visual Servoing," In:D. Rus and S. Singh (Eds), *Experimental Robotics VII*, Springer–Verlag, pp. 169–178, 2001.

[4] R. Kelly, R.Carelli, O. Nasisi, B. Kuchen and F. Reyes, "Stable Visual Servoing of Camera-in-Hand Robotic Systems," *IEEE/ASME Trans. Mechatronics*, vol. 5, no. 1, pp. 39-48, 2000.

[5] H. Kobayashi *et al.*, *Practical Control of Robot Manipulators*, Corona Publishing Co., 1997.

[6] A. Maruyama, H. Kawai and M. Fujita, "Stability and Tracking Performance of Dynamic Visual Feedback Control for Nonlinear Mechanical Systems," *Proc. of the 40th IEEE Conference on Decision and Control*, pp. 4415-4420, 2001.

[7] A. Maruyama, H. Kawai and M. Fujita, "Passivity-based Visual Feedback Control of Nonlinear Mechanical Systems –Stability and L_2-Gain Performance Analysis," *Trans. Institute of Systems, Control and Information Engineers*, vol. 15, no. 12, pp. 627–635, 2002.

[8] R. Murray, Z. Li and S. S. Sastry, *A Mathematical Introduction to Robotic Manipulation*, CRC Press, 1994.

[9] F. Bullo and R. Murray, "Tracking for Fully Actuated Mechanical Systems : A Geometric Framework," *Automatica*, vol. 35, no. 1, pp. 17–34, 1999.

[10] A. van der Schaft, *L_2-Gain and Passivity Techniques in Nonlinear Control* (2nd ed.), Springer–Verlag, 2000.